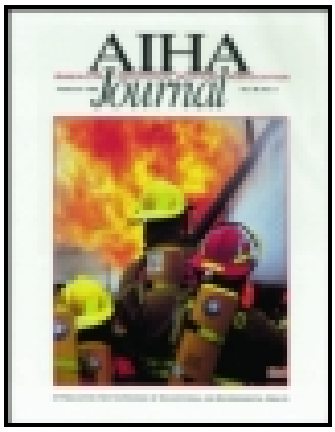

American Industrial Hygiene Association Journal
Publication details, including instructions for authors and subscription information:
http://www.tandfonline.com/loi/aiha20

LOADING AND FILTRATION CHARACTERISTICS OF FILTERING FACEPIECES

C. C. Chen [a] , M. Lehtimäki [a] & K. Willeke [a]
[a] Aerosol Research and Respiratory Protection Laboratory, Department of Environmental Health, University of Cincinnati, Cincinnati, OH 45267-0056
Published online: 04 Jun 2010.

To cite this article: C. C. Chen , M. Lehtimäki & K. Willeke (1993) LOADING AND FILTRATION CHARACTERISTICS OF FILTERING FACEPIECES, American Industrial Hygiene Association Journal, 54:2, 51-60, DOI: 10.1080/15298669391354324

To link to this article: http://dx.doi.org/10.1080/15298669391354324

Loading and Filtration Characteristics of Filtering Facepieces

C. C. Chen, M. Lehtimäki[1]
K. Willeke

Aerosol Research and Respiratory Protection Laboratory, Department of Environmental Health, University of Cincinnati, Cincinnati, OH 45267-0056

Most filtering facepieces used today are made of electret material (material with significant electrical charges on the filter fibers). Because of the addition of this electrical removal force, the filtration efficiency can be significantly increased without increasing the air pressure drop inside the respirator; pressure drop is closely related to physiological load. However, the removal by electrical forces is reduced in time, as aerosols deposit on the filter fibers. We have studied the contribution of this electrical removal and its change in time as a function of aerosol loading. To prove the change in aerosol penetration is due to the reduction of electrical force, the electrical charges were removed from new facepieces by the application of appropriate chemicals.

The dust-mist filtering facepieces tested have similar fiber diameters and packing densities, as determined by scanning electron microscopy and pressure drop data. At a face velocity of 10 cm/s (corresponding to 100 L/min through a complete filtering facepiece) and an aerosol size of 0.16 μm, electrical force removal accounts for 69% of the total filtration for the respirator found to have the best filter quality but only 25% for the respirator (from a different manufacturer) found to have the worst filter quality. Our experimental data show that the removal efficiency of these facepieces is reduced in time by as much as this amount. However, under normal wear conditions, the total aerosol particle load is not as high as shown and the filtering facepieces are likely to be discarded before the fiber charges (i.e., the electrostatic attractions) are significantly diminished.

For decades, respirators and air pollution devices have used fibrous filters to remove particulate matter and improve air quality. When filtering to meet air quality criteria, one must consider the minimum filtration efficiency required and the air resistance. High resistance may result in increased operation and maintenance costs. When selecting a respirator, one must consider the same parameters, filtration efficiency and air resistance, with an additional condition: the air resistance must be tolerable to humans. The human body has very limited respiration capacity and high air resistance may present a significant burden to the wearer, especially in the case of long-term use.

Filtering facepieces have many advantages over elastomeric respirators with cartridges: less maintenance, easier communication with co-workers, less burden and less vision obstruction. For these reasons, workers generally prefer filtering facepieces to elastomeric respirators.

A filtering facepiece normally has a surface area of about 165 cm^2. Elastomeric respirators normally have two cartridges. In HEPA cartridges the filter material is usually pleated inside resulting in a total surface area of about 400 cm^2 for the two cartridges. Therefore, an elastomeric respirator theoretically performs better than a filtering facepiece if the same filter material is used because the larger surface area provides not only lower air resistance but also more filter material to collect the aerosols.

In our recent study[(1)] on aerosol penetration through commercially available, MSHA/NIOSH approved respirators, some of the cartridges performed worse than some of the filtering facepieces of the same category, although the cartridges contained a larger filtration surface area. We also found considerable differences in the performance of filtering facepieces of the same category. The best dust-mist filtering facepiece provided over five times more protection than the worst one tested.

In the present study, we investigated why respirators of the same category perform so differently. The degradation of collection efficiency by aerosol loading was also investigated. Some filtering facepieces of a higher performance category are made up of several layers of the same material used for a lower category filtering facepiece. We have investigated the cumulative effect of multiple filtration layers on pressure drop and filtration efficiency.

BACKGROUND

Filtration mechanisms have been studied in great detail. Many theories have been developed using models of flow patterns

[1]On leave from Technical Research Centre of Finland, P.O. Box 656, SF-33101 Tampere, Finland.

around the fiber.[2] There are five known filtration mechanisms which contribute to aerosol filtration: diffusion, interception, impaction, gravitational settling and electrostatic attraction.

Many studies[3–10] have focused on diffusion, interception and/or impaction simultaneously because these mechanisms interact with each other and the sum of their individual contributions to performance does not always equal the actual performance measured. Particle deposition by diffusion is a random process that occurs due to the particle's interaction with the random motion of the air molecules. It increases with decreasing particle size and decreasing face velocity (flow rate divided by the cross-sectional area of the filter surface). Deposition by interception occurs when an aerosol particle follows the air streamline within one particle radius of the surface of the fiber. It is the only one of the five mechanisms which is not affected by the face velocity. Interception is proportional to the ratio of particle diameter to fiber diameter. Deposition by impaction occurs when an aerosol particle deviates from the streamline and hits the fiber. Impaction depends on the mass and velocity of the particle and somewhat on its shape. The effect of this mechanism increases with increasing face velocity, particle diameter and particle density. Gravitational settling is normally negligible in respirator filtration because the settling velocity is insignificant compared to the face velocity.

The mechanism of electrostatic attraction can be significant. Therefore, most filtering facepieces are made of electret material, i.e. electrically charged fibers, which enhance the aerosol capture efficiency without increasing the air resistance. Electrostatic attraction depends on the degree to which the fibers and the aerosol particles are electrically charged.[11–16] Charged aerosol particles deposit on the charged fibers because of Coulombic and induced dielectrophoretic forces.

As aerosol particles deposit on the filter, the effective fiber diameter and the packing density (ratio of fiber to filter volume) increase. With this increase in material onto which the particles may deposit, the mechanical removal efficiency due to interception, impaction and diffusion is expected to increase, i.e. less particles should penetrate through the filter with time, as shown in studies of industrial electret filters.[17,18] In our study, we have examined the effect of loading respiratory filtering facepieces.

In studies on industrial electret filters, some chemicals, such as distilled water, sodium chloride solution, and ethanol have been used to reduce the fiber charge.[19] Kanaoka et al. found that an industrial electret filter treated with ethanol had a significant increase in aerosol penetration, indicating that some of the fiber charges were removed.[19] In our study, more efficient chemicals were used to remove the electrical charges on the filters in order to investigate the enhancement of particle removal by electrostatic attraction.

THEORETICAL ESTIMATION OF FILTRATION EFFICIENCY

We experimentally determined the aerosol penetration for several brands of filtering facepieces. The experimental penetration data are compared to theoretical predictions. This comparison was done macroscopically (entire filtering facepiece) and microscopically (single fiber).

Macroscopically, the filtering facepiece is made of three layers: the cover web outside, the support shell inside and the filtration layers in the middle. The filtration layers are responsible for most of the aerosol filtration and the air resistance. Filter penetration exponentially decreases as the number of filtration layers increases because the filtration layers are independent of each other when the aerosol particles deposit uniformly throughout the filter material, i.e. when caking does not occur. Thus, the penetration efficiency for m filtration layers, P_m is multiplicative:

$$P_m = (P_1)^m \quad (1)$$

where P_1 is the aerosol penetration of a single filtration layer.

The pressure drop across the respirator filter increases linearly with an increase in the number of filtration layers because the air flow through the respirator is laminar. Thus the pressure drop across m filtration layers, Δp_m, is additive:

$$\Delta p_m - m\Delta p_1 \quad (2)$$

where Δp_1 is the pressure drop across a single filtration layer.

Microscopically, single fiber theories are normally used to calculate the total capture efficiency.[20] Aerosol penetration, P_n, for a particle with n elementary charges is given by

$$P_n = \exp\left(\frac{-4\alpha x E_{\Sigma,n}}{\pi d_f}\right) \quad (3)$$

where α is the packing density; d_f is the fiber diameter; x is the filter thickness; and $E_{\Sigma,n}$ is total single fiber filtration efficiency (of a particle with n elementary charges) due to the combined effect of several filtration mechanisms:

E_d is the single fiber efficiency due to diffusional deposition; E_r is

$$E_{\Sigma,n} = f(E_d, E_r, E_i, E_g, E_p, E_{c,n}) \quad (4)$$

due to interception; E_i is due to impaction; E_g is due to gravitational settling; E_p is due to the dielectrophoretic force; and $E_{c,n}$ is due to the Coulombic force.

The single fiber filtration efficiency due to diffusional deposition[7] is given by

$$E_d = 2.6\left(\frac{1-\alpha}{k}\right)^{1/3} Pe^{-2/3} \quad (5)$$

where K is the Kuwabara factor and Pe is the dimensionless Peclet number. The Kuwabara factor is a function of packing density α (also called solidity):

$$K = -\left(\frac{1}{2}\right)\ln\alpha - 0.75 + \alpha - \left(\frac{1}{4}\right)\alpha^2 \quad (6)$$

The Peclet number relates the diffusional transport of particles to the filter to the macroscopic flow, indicated by face velocity v (before entering the filter):

$$Pe = \frac{d_f v}{D} \quad (7)$$

where D is the aerosol diffusion coefficient.

The single fiber filtration efficiency due to interception[7] is represented by

$$E_r = \left(\frac{1-\alpha}{K}\right)\left(\frac{R^2}{1+R}\right) \quad (8)$$

where R is the ratio of particle diameter, d_p, to fiber diameter, d_f:

$$R = \frac{d_p}{d_f} \quad (9)$$

In our calculations comparing our experimental data to theoretical predictions we have represented the single fiber efficiency for impaction by[20]

$$E_i = \frac{(Stk)J}{2K^2} \quad (10)$$

where Stokes number, Stk, relates the particle's inertial stopping distance to the filter diameter and is defined as:

$$Stk = \frac{\rho_p d_p^2 C_c v}{18\eta d_f} \quad (11)$$

The density of the particle is represented by ρ_p (e.g., 0.95 g/cm^3 for corn oil), C_c is the Cunningham correction factor, η is the viscosity of air ($1.81 \cdot 10^{-5}$ Pa/sec at normal temperature and pressure) and J is:

$$J = (29.6 - 28\alpha^{0.63})R^2 - 27.5R^{2.8} \quad (12)$$

The single fiber filtration efficiency caused by aerosol gravitational settling[20] is given by

$$E_g = \frac{\rho_p d_p^2 C_c g}{18\eta v} \quad (13)$$

which represents the ratio of the particle's gravitational settling velocity to the face velocity of the flow through the filter.

The single fiber filtration efficiency due to the interaction between a polarized charged fiber and an aerosol particle[16] is given by

$$E_p = \left(\frac{1-\alpha}{K}\right)^{2/5} \frac{\pi N_d}{1 + 2\pi N_d^{2/3}} \quad (14)$$

N_d is a dimensionless parameter:

$$N_d = \frac{\varepsilon_p - 1}{\varepsilon_p + 2} \frac{2\sigma^2 d_p^2 C_c}{3\varepsilon_0 (1+\varepsilon_f)^2 \eta d_f v} \quad (15)$$

where ε_f is the dielectric constant of the aerosol (2.2 for corn oil); ε_f is the dielectric constant of the fiber (2.5 for polypropylene); ε_0 is the dielectric constant in vacuum ($8.8544 \cdot 10^{-12}$ C^2/Nm^2); and σ is the fiber charge density.

The single fiber filtration efficiency due to the Coulombic force between a charged fiber and an aerosol particle with n elementary charges[16], $E_{c,n}$, is given by

$$E_{c,n} = \left(\frac{1-\alpha}{K}\right)^{1/8} \frac{\pi N_{c,n}}{1 + 2\pi N_{c,n}^{1/4}} \quad (16)$$

where $N_{c,n}$ is a dimensionless parameter related to the number of electrons with charge e ($1.6 \cdot 10^{-19}$ C or $4.8 \cdot 10^{-10}$ electrostatic units).

$$N_{c,n} = \frac{ne\sigma C_c}{3\pi\varepsilon_0(1+\varepsilon_f)\eta d_p v} \quad (17)$$

Summation of all of the single fiber filtration efficiencies may result in an overestimation of the total single fiber filtration efficiency because the different filtration mechanisms may compete for the same particle.[20] Most of the interactions among these mechanisms have not yet been quantified and direct summation had to be used assuming there is no interaction.[16] We have, however, taken into account the interaction of diffusion and interception[7] through the combined single fiber filtration efficiency for diffusion and interception, E_{dr}:

$$E_{dr} = 1.6\left(\frac{1-\alpha}{K}\right)^{1/3} Pe^{-2/3} + 0.6\left(\frac{1-\alpha}{K}\right)\frac{R^2}{1+R} \quad (18)$$

The single fiber filtration efficiency caused by all of the mechanical filtration mechanisms, E_m, is related to the penetration efficiencies of these mechanisms and has been represented by

$$E_m = 1 - (1 - E_{dr})(1 - E_i)(1 - E_g) \quad (19)$$

where E_{dr} is obtained from Equation 18, E_i from Equation 10, and E_g from Equation 13.

The single fiber filtration efficiency, $E_{e,n}$, for the two electrical filtration mechanisms has been determined by direct summation:

$$E_{e,n} = E_p + E_{c,n} \quad (20)$$

where E_p is obtained from Equation 14, and $E_{c,n}$ is calculated using Equation 16.

The total single fiber filtration efficiency is then calculated by adding the combined electrical single fiber efficiency to the mechanical efficiency:

$$E_{\Sigma,n} = E_m + E_{e,n} \quad (21)$$

Equation 21 has been used in Equation 3 to calculate the aerosol particle penetration for each charge level. We neutralized the challenge aerosols to Boltzmann equilibrium. Thus, the aerosol particle penetration P is:

$$P = B(0)\exp\left(\frac{-4\alpha x E_{\Sigma,0}}{\pi d_f}\right) + 2\sum_{n=1}^{\infty} B(n)\exp\left(\frac{-4\alpha x E_{\Sigma,n}}{\pi d_f}\right) \quad (22)$$

B(n) is the Boltzmann distribution:

$$B(n) = \frac{2e}{\sqrt{\pi d_p kT}} \exp\left(\frac{-n^2e^2}{d_p kT}\right) \quad (23)$$

where k is the Boltzmann constant ($1.38 \cdot 10^{-16}$ dyn • cm/K) and T is the absolute temperature (298 K in our calculations).

Experimental Material and Methods

Eight filtering facepieces of different category (1 nuisance dust, 4 dust-mist, 2 dust-mist-fume and 1 HEPA) were challenged with corn oil aerosol for 8 hours to study the loading effect. A dynamic measurement system (discussed further below) continuously measured the effect of loading on the pressure inside and aerosol penetration through the filtering facepieces.

Three filtering facepieces made of the same filtration material were chosen to study the cumulative effect of multiple filtration layers: a dust-mist respirator (MSHA/NIOSH approved) with one filtration layer; a CEN P2 respirator (used in Europe, regulated by the European Committee for Standardization) with 4 filtration layers; and a HEPA respirator (MSHA/NIOSH approved) with 6 filtration layers. The filtering facepieces (made by the same company) were sealed to a mannequin to measure the air resistance and the penetration of aerosol particles.

We chose the best and the worst dust-mist filtering facepieces, based on our previous study,[11] to investigate what makes respirators (of the same defined category) perform differently. Either isopropanol (class 1B, Fisher Scientific, Fair Lawn, NJ) or static guard (Alberto- Culver Company, Melrose Park, IL) was applied to the facepieces to reduce (or mask) the fiber charges. The respirators were immersed in either of these chemicals for one hour and were then dried naturally for 24 hours. A portion of each filtering facepiece was installed in a filter holder (model 2200, Gelman Sciences, Inc., Ann Arbor, MI). The effective filtration area was measured to be approximately 13.2 cm^2. The air flow was adjusted to a face velocity of 10 cm/sec, corresponding to an instantaneous inhalation flowrate of about 100 L/min. A Collison nebulizer was used to load the filter with corn oil aerosol having a count median diameter of about 0.6 μm and a geometric standard deviation of about 1.8. Each filter was loaded with up to 40 mg/cm^2 of corn oil, assumed to coat the fibers uniformly. After loading, the respirator piece was weighed using an analytical balance and was then placed in the test chamber (held in the same filter holder) to measure the aerosol penetration. This process was repeated until the filter became clogged.

Two corn oil aerosols were used in this study: A loading aerosol and a challenge test aerosol. The loading aerosol was produced with the Collison nebulizer to coat the fibers as described above. The challenge test aerosol was used to measure the aerosol penetration through the filter. The design and characterization of the challenge aerosol generation and sampling system used in this study have been described in detail elsewhere.[11] A newly developed size-fractionating aerosol generator[22,23] delivered the corn oil test aerosol with a selected size distribution. The aerosol was neutralized to Boltzmann charge equilibrium using a 10 mCi Kr 85 radioactive source. Filtered dilution air flow carried the aerosols to the test chamber. The aerosol concentrations before and after filtration were sized by an Aerodynamic Particle Sizer (model APS33B, TSI Inc., St. Paul, MN) and a Laser Aerosol Spectrometer (model LAS-X CRT, PMS Inc., Boulder, CO). The optical particle size recorded by the latter instrument was converted to physical size by calibration with an Electrical Aerosol Classifier (model 3071, TSI Inc., St. Paul, MN) and then into aerodynamic size through knowledge of the density

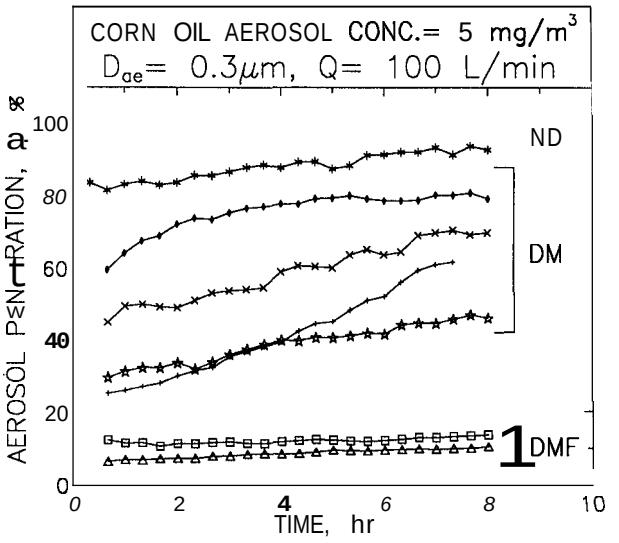

FIGURE 1. Aerosol penetrations of 7 filtering facepieces. ND: nuisance dust respirator. DM: dust-mist respirator. DMF: dust-mist-fume respirator

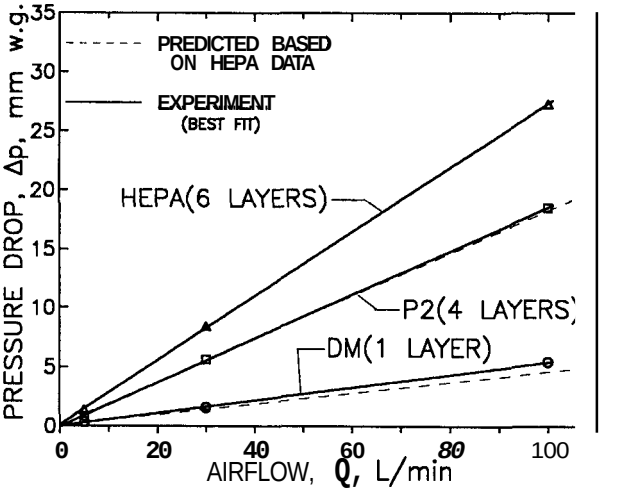

FIGURE 2. Effect of the number of filtration layers on pressure drop across filtering facepieces. DM: dust-mist respirator (1 filtration layer). P2: respirator regulated by European Standard (4 filtration layers). HEPA: high efficiency respirator (6 filtration layers)

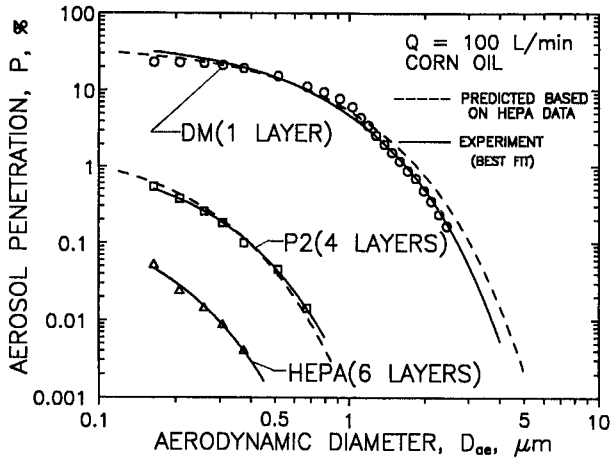

FIGURE 3. Effect of the number of filtration layers on aerosol penetration

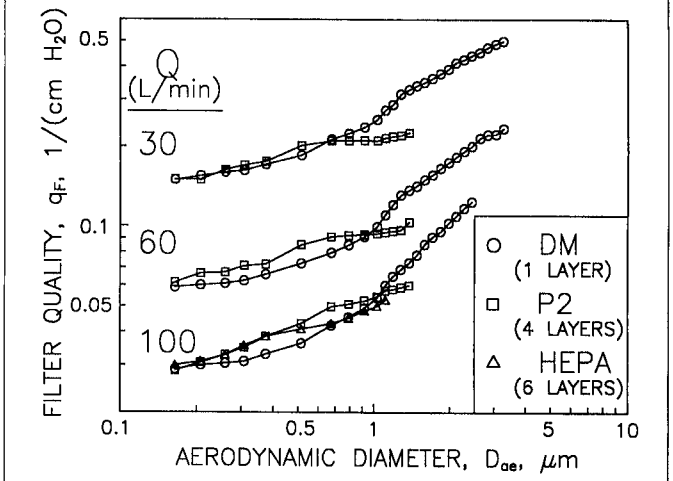

FIGURE 4. Effect of the number of filtration layers on the filter quality factor

of the test aerosol (ρ_p = 0.95 g/cm^3 for corn oil). The air flows were controlled by a mass flow controller (model 247C, MKS Instruments Inc., Andover, MA). The pressure drop across the respirator filter was measured using an inclined manometer.

RESULTS AND DISCUSSION

The aerosol penetration increases with time for all filtering facepieces tested, as shown in Figure 1. Each line connects the data obtained with different brands of filtering facepieces. The data for the HEPA filtering facepieces are not shown because the percentage of aerosol penetration is close to zero. The indicated flowrate, Q, of 100 L/min simulates an inhalation rate of that magnitude. This corresponds to a breathing rate of about 50 L/min or less. During exhalation, no contaminants penetrate from outside to inside the respirator. The flowrate of 100 L/min is the highest flowrate tested and simulates a heavy work load.

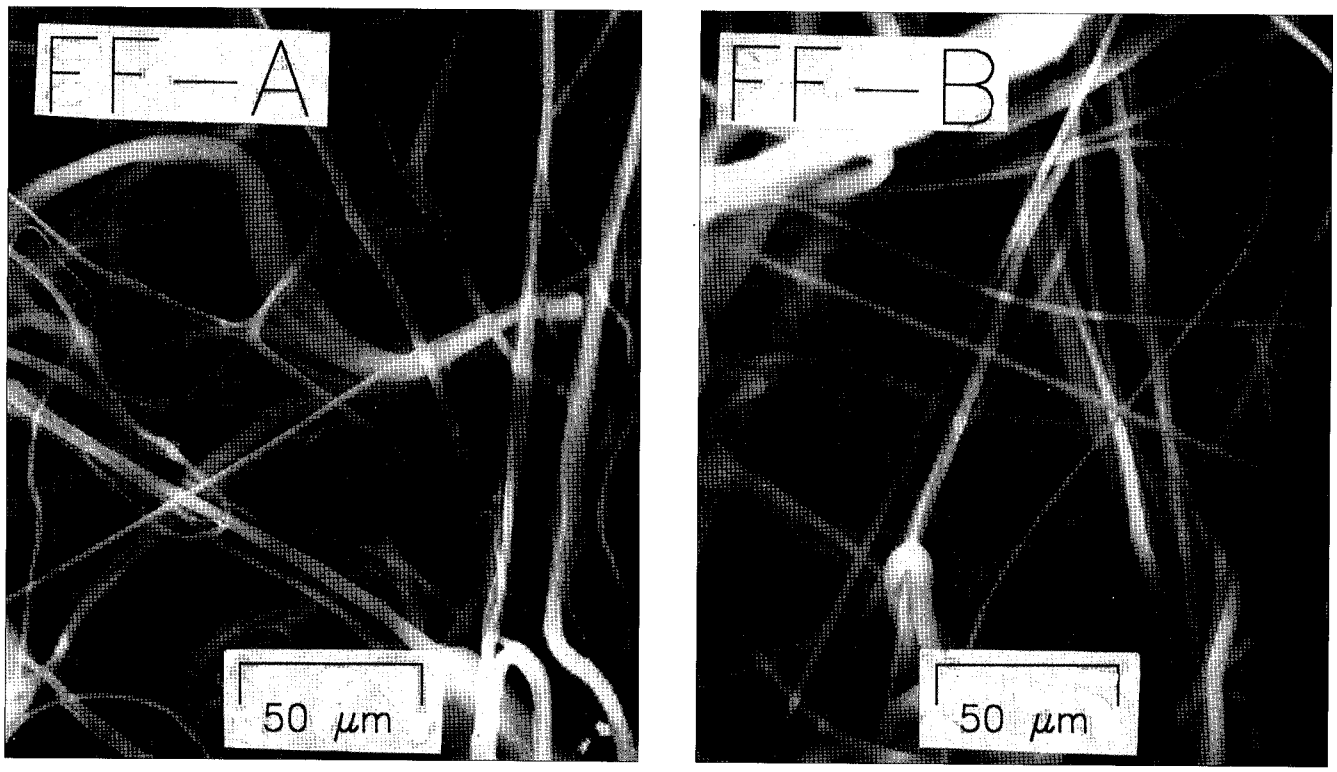

FIGURE 5. Scanning electron micrographs of the filtration layer in two dust-mist filtering facepieces. Mean fiber diameter ≃ .2 μm

The data of Figure 1 are shown for particles with an aerodynamic diameter, D_{ae}, of 0.3 μm. Particles of other submicrometer sizes have similar increases in aerosol penetration with time. This increase with time suggests that all of the tested facepieces carry some degree of electrical charge on their fibers and that particle removal by electrical attraction accounts for a significant fraction of aerosol particle removal in filtering facepieces. As the fibers get coated by the particles—liquid corn oil aerosol particles in this case, used conventionally in fit testing—the electrical charge on the fibers is shielded and becomes less effective in attracting particles. Performance evaluations of industrial electret filters have shown similar increases in aerosol penetration.[17,18]

The effect of the number of filtration layers on pressure drop and aerosol penetration was examined first. Macroscopically, the pressure drop across the facepieces increased linearly with airflow (see Figure 2), indicating that the flow is laminar. For instance, the pressure drop across the HEPA respirator is 1.35 mm H_2O at 5 L/min, 8.1 mm H_2O at 30 L/min, and 27 mm H_2O at 100 L/min. Because of the presence of a cover web and a support shell, the correlation of Equation (2) is not perfect. Since the pressure drop data of the HEPA filter are affected the least by the cover web and the support shell, the pressure drop data across the HEPA filter were used to predict the pressure drops across the P2 and DM respirators. Figure 2 shows reasonable agreement between the expected and experimental values.

Figure 3 shows that the aerosol penetration exponentially decreases with the number of filtration layers. The HEPA filtering facepiece has the thickest filtration layer; thus, the aerosol penetration through the HEPA facepiece is least affected by the cover web and the support shell. We used Equation 1 and the aerosol penetration curve for the HEPA facepiece to predict the aerosol penetrations through the other respirators with less filtration layers. The differences between the best fit curves for the experimental data and the predicted curves are probably caused by the additional particle removal in the cover web and the support shell. The validity of Equation 1 for different particle sizes deserves further study.

If the number of filtration layers affects aerosol penetration in a multiplicative way, Equation 1, and pressure drop in an additive way, Equation 2, then the logarithm of the aerosol penetration should be related to the linear pressure drop for a given flowrate and particle size. This can be expressed through the filter quality factor, q_F, defined as

$$q_F = \frac{\ln\left(\frac{1}{P}\right)}{\Delta p} \qquad (24)$$

As seen in Figure 4, q_F is approximately the same for each facepiece tested at a given flowrate. The dust-mist facepiece has a somewhat higher q_F for particles above 1 μm, because the additional particle removal by the web and shell has the greatest effect on this factor when only one filtration layer is used. The filter quality for the HEPA filtering facepiece was determined only at the 100 L/min mask flow because the particle count inside the facepiece was insufficient at the lower flow rates. The filter quality for the P2 filtering facepiece is not shown for particle sizes larger than 1.2 μm for the same reason.

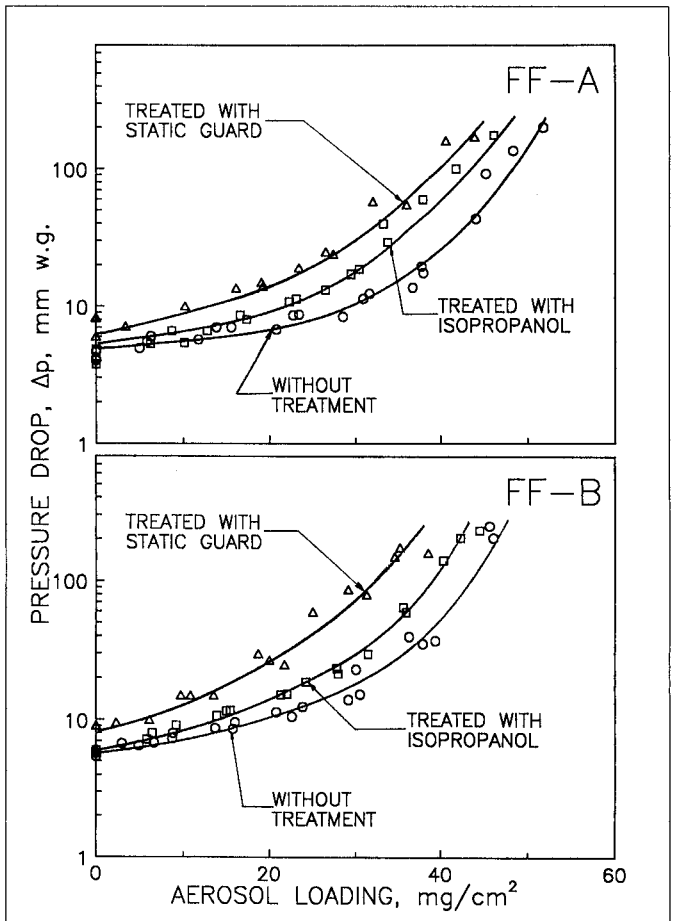

FIGURE 6. Pressure drop as a function of aerosol loading for two brands of dust-mist filtering facepieces. Face velocity = 10 cm/sec

Two dust-mist filtering facepieces were chosen to examine the difference in performance of respirators in the same category. These are identical with filtering facepieces A and D in Figure 5 of reference 1. The best performing facepiece will be referred as FF-A and the worst as FF-B. Scanning electron micrographs of the filtration layers of the two facepieces, Figure 5, indicate that both have approximately the same mean fiber diameter of about 2 μm, the same distribution of fiber diameters, and the same porosity. Their mechanical filtration efficiencies should, therefore, be similar to each other.

The pressure drop across the dust-mist filtering facepieces was examined first. The pressure drop is affected only slightly by the structure for a given packing density and fiber diameter.[24,25] Figure 6 shows that FF-A and FF-B induce about the same pressure drop when tested as received. As the filter material is loaded with aerosol particles, the pressure drop increases for each respirator in a similar manner. In respirator wear, the facepieces are discarded before excessive aerosol loading is achieved, because the pressure drop becomes unacceptable. The OSHA-regulated maximum allowable resistance requirements for DM respirators, at a

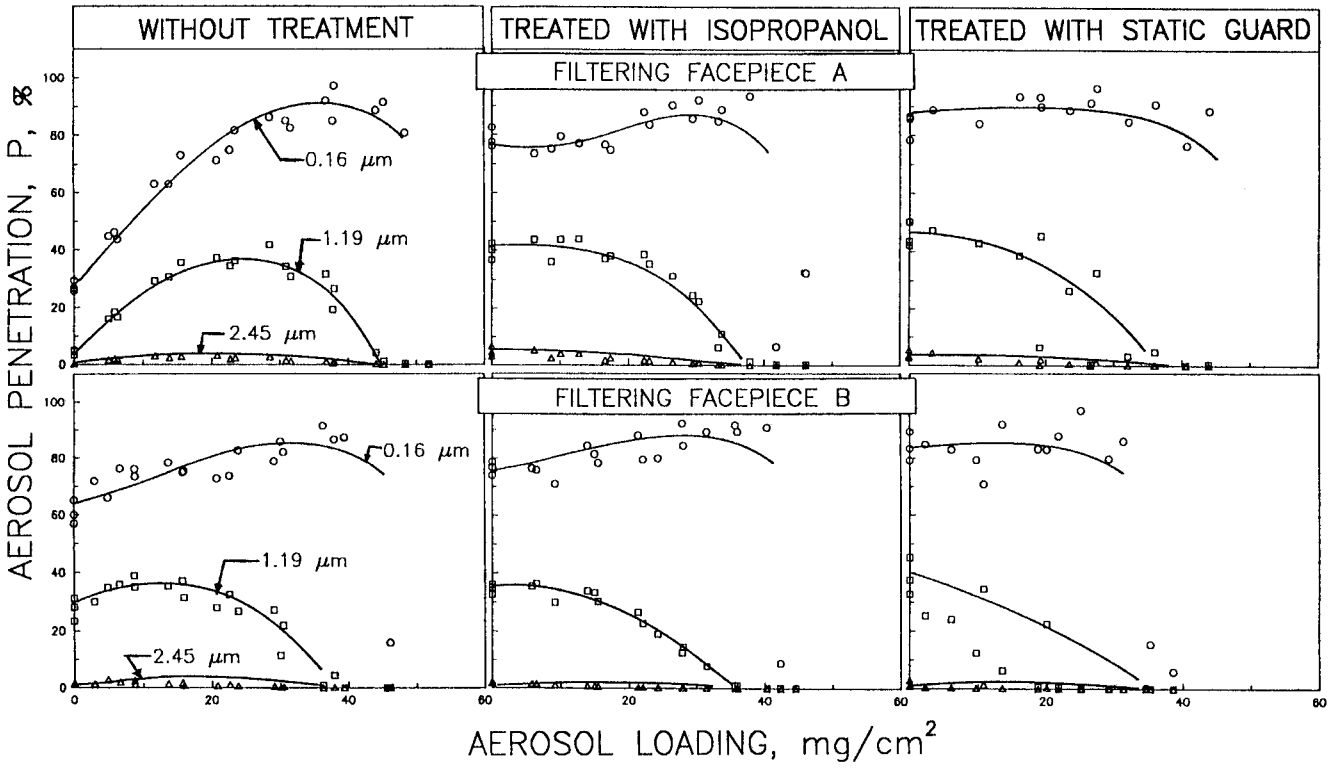

FIGURE 7. Change in aerosol penetration due to reduction in fiber charge upon loading by aerosols. Face velocity = 10 cm/sec

continuous airflow of 32 L/min after the silica test, are 30 mm H_2O at initial inhalation, 50 mm H_2O at final inhalation and 20 mm H_2O at exhalation.[26] The similarity in performance indicates that the two filtering facepieces tested have approximately the same packing density, since they have the same mean fiber size. The chemically treated filters have a higher initial pressure drop. This may occur if particles deposit on the fibers, thereby decreasing the porosity, or if the structure of the filter is modified after the chemicals evaporate. We did not observe a significant increase in fiber diameter under the microscope. It appears that the surface tension of the liquid pulls the fibers together during drying, thus reducing the thickness of the filter and increasing its packing density. The initial packing density of the two dust-mist filtering facepieces was estimated to be about 0.05.

Electrically charged filters (electrets) are normally very stable, lasting for years.[2] However, the fiber charge is reduced and the performance decreases when electret filters are exposed to high humidity, high temperature, industrial aerosols, or some chemicals.[17,19] Isopropanol and static guard were found to be capable of removing almost all the fiber charges. This is demonstrated in Figure 7. For filters without any chemical treatment, the aerosol penetration first increases with aerosol loading because of the reduction of the electrical force due to fiber coating. With further aerosol loading, the aerosol penetration decreases because of the filter's increased packing density. Ultimately, the filter clogs and aerosol penetration approaches zero. For instance, for FF-A, the maximum penetration is 92% for 0.16 μm aerosols at a load of about 38 mg/cm^2 and 37% for 1.19 μm aerosols at a load of 27 mg/cm^2. The 0.16 μm size was chosen to represent the aerosol penetration behavior in the submicrometer-sized range, where the electrical forces may dominate. The two supermicrometer sizes were chosen to represent sizes for which other particle removal mechanisms, such as interception, are significant. The corn oil challenge aerosol was polydisperse with a count median diameter of 1.9 μm and a geometric standard deviation of 1.7 (measured by the Aerodynamic Particle Sizer).

The initial increase and subsequent decrease of aerosol penetration also occurs with 2.45 μm aerosols. Aerosol penetration for this size (when examined on a logarithmic ordinate) decreases significantly after the maximum penetration point. The larger aerosol particles are apparently blocked from passing through the filter before the smaller ones are. Because of the low packing density of the respirator filter neither FF-A nor FF-B clogs easily when loaded with liquid aerosols which uniformly coat the fibers. Figure 7 shows that both FF-A and FF-B have considerable loading capacity (20 to 40 mg/cm^2) for submicrometer-sized aerosols. As shown previously in Figure 6, such loading densities are never achieved in respirator wear, because the pressure drop becomes excessive. Figure 7 is shown here to prove the importance of aerosol particle removal by electrical attraction forces.

For a chemically treated filter, the initial aerosol penetration is very close to the maximum aerosol penetration of an untreated filter after loading. This indicates that most of the fiber charges have been removed during the chemical treatment. Static guard appears to have removed the fiber charges

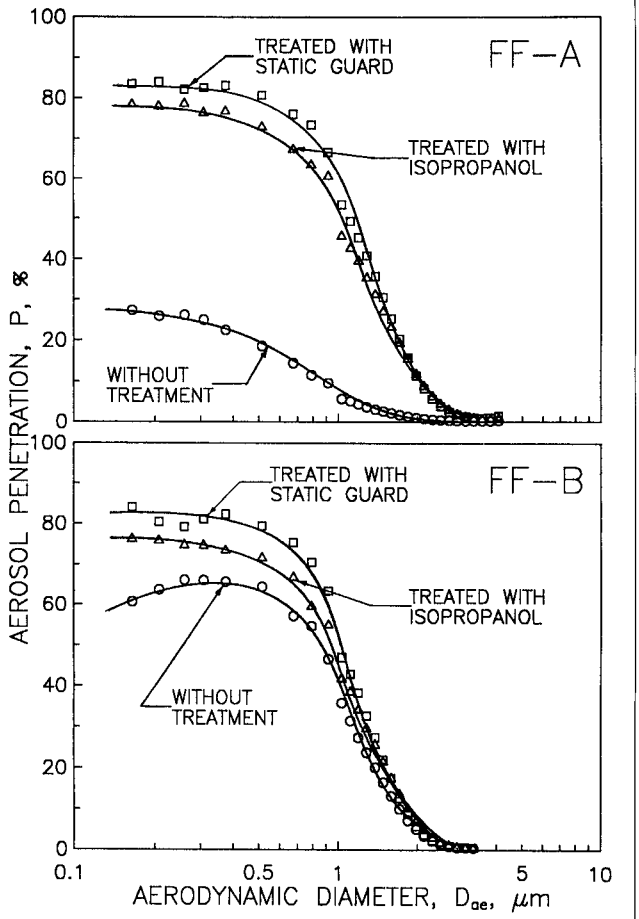

FIGURE 8. Particle size dependence of penetrated aerosols for dust-mist filtering facepieces at the beginning of a loading cycle with corn oil aerosols. Face velocity = 10 cm/sec

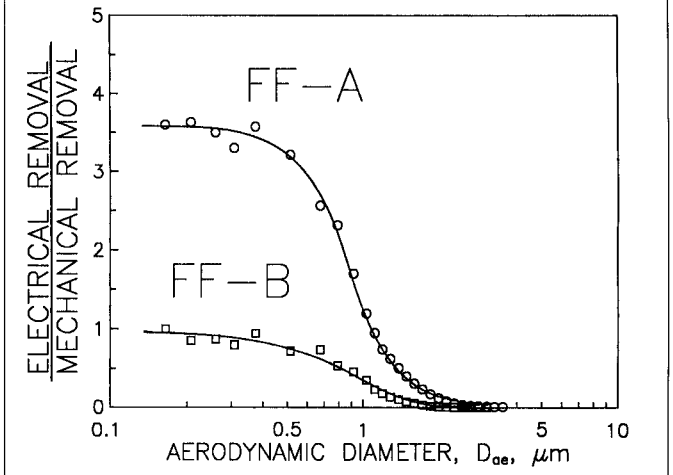

FIGURE 9. Aerosol particle removal by electrical versus mechanical forces. Face velocity = 10 cm/sec

more effectively than isopropanol. No increase in aerosol penetration is observed for filters treated with static guard. The curves of Figure 7 are approximate fits to the data points and have been drawn to indicate the increases and decreases in aerosol penetration.

The aerosol penetrations at the beginning of a loading cycle are shown as a function of particle size in Figure 8. After chemical treatment to remove the electrical charges from the fibers, FF-A and FF- B have almost the same penetration patterns. This again proves that FF- A and FF-B have about the same mechanical properties: similar fiber diameters and packing density. At the beginning of wear, FF-A clearly has much lower aerosol penetration than FF-B.

The aerosol particle removal percentages (100 - penetration %) of Figure 8 have been used to calculate the relative importance of aerosol particle removal by electrical versus mechanical forces, as shown in Figure 9. Since static guard appears to have removed the charges more effectively than isopropanol, the curves for static guard in Figure 8 have been used. For submicrometer-sized aerosols, aerosol particle removal by electrical forces is 3.5 times greater than by mechanical forces for FF-A. For FF-B both forces have about the same removal efficiency. For supermicrometer-sized aerosols, mechanical force removal is higher than electrical force removal. At lower face velocities, electrical force removal is expected to be relatively higher for 1 μm particles because of the particles' increased time of passage through the filter which gives the electrical forces more time to act on the particles.

The experimental data were also analyzed by calculating the aerosol particle removal efficiencies for all the forces that may act on the particles in the filters under consideration. Figure 10 shows the single fiber filtration efficiencies of dipole fibers when collecting aerosols neutralized to Boltzmann charge equilibrium. Figure 10 shows that dielectrophoretic attraction (resulting in single fiber filtration efficiency, E_p, Equation 14) is the primary collection mechanism for singly charged aerosol particles in the size range of about 0.2 to 5 μm. Interception (E_r, Equation 8) is the primary mechanical filtration mechanism for aerosol particles larger than 0.3 μm but smaller than 1.5 μm. Coulombic attraction ($E_{c,1}$, Equation 16) is greater than diffusion (E_d, Equation 5) for the indicated conditions. Both E_c and E_d contribute significantly when the aerosol particle is less than about 0.2 μm, but their contributions decrease with increasing aerosol size. The contributions by impaction (E_i, Equation 10) and gravitational settling (E_g, Equation 13) increase with increasing aerosol size. E_g is not significant when compared to the other filtration mechanisms.

The total single fiber efficiency on aerosol particles with n elementary charges ($E_{\Sigma,n}$, Equation 21) has been calculated by summing the total mechanical single fiber efficiency (E_m, Equation 19) to the electrical single fiber efficiency ($E_{e,n}$, Equation 20). $E_{\Sigma,n}$ has then been used to calculate aerosol penetration, Equation 22, for aerosols in Boltzmann charge equilibrium and exposed to a filter of thickness x = 0.4 mm.

Figure 11 shows the results of the calculations applied to the two filtering facepieces used in this study. The thin solid lines are the calculated mechanical penetration efficiencies for the measured packing density α = 0.05 and electron-mi-

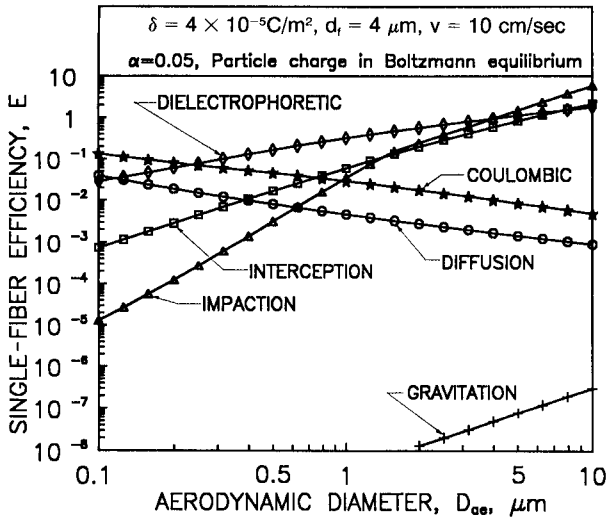

FIGURE 10. Theoretical single fiber efficiency for a dipole fiber. δ: fiber charge density. d_f: fiber diameter. a: packing density. v: face velocity. The indicated charge density corresponds to dust-mist filtering facepiece FF-A

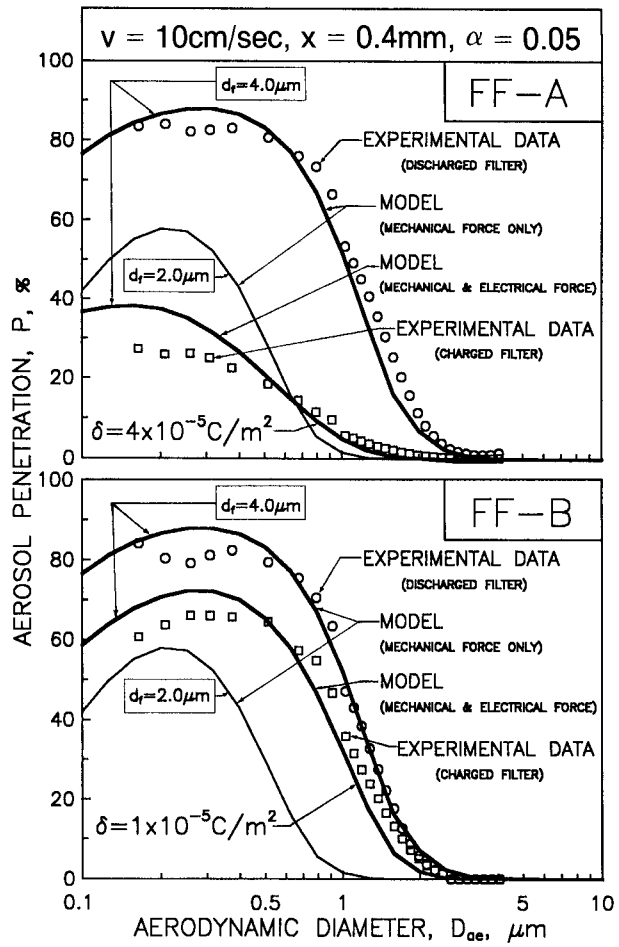

FIGURE 11. Comparison of theoretical calculations to experimental data for the best and worst performing dust-mist filtering facepieces. x: filter thickness

croscopically measured mean fiber diameter of 2 μm. As seen, these modelled penetration efficiencies are less than the experimentally determined mechanical efficiency data. Single fiber efficiency calculations generally do not match the experimental data, because the fibers are usually not of the same size and are not uniformly distributed. During the manufacturing process, fibers easily cluster and form equivalent larger fibers. Some investigators have accounted for this nonuniformity in the distribution of fibers in the media by introducing an inhomogeneity factor in the exponential of Equation 3.[27] This inhomogeneity factor can be defined in terms of pressure drop or single fiber efficiency. However, this approach may not totally match the theoretical values to the experimental ones, since most of the interactions among individual single-fiber filtration mechanisms have not been quantified. Therefore, we back-calculate an equivalent fiber size from the penetration data. For our data, the equivalent fiber diameter is 4.0 μm for the measured packing density of 0.05. With these equivalent values, the single fiber efficiency calculation matches the experimental data for mechanical removal quite well, as seen by the upper solid lines in Figure 11. The electrical charge on the filters has then been calculated by matching the single fiber efficiency calculation for mechanical and electrical removal to the experimental data for the chemically untreated filter. The fiber charge densities for FF-A and FF-B were thus determined to be 4×10^{-5} and 1×10^{-5} C/m^2 respectively, i.e. FF-A has 4 times fiber charge of FF-B. FF-A also removes 5 times more aerosol mass than FF-B, when exposed to a regulated test dust.[1]

CONCLUSIONS

In theory, air resistance of respirator filters increases linearly with increasing filter thickness and aerosol penetration decreases exponentially with increasing filter thickness. In practice, however, these relationships are not perfectly linear or exponential but are influenced by added pressure drop and aerosol removal in the cover web and support shell.

Chemicals, such as isopropanol and static guard, remove most of the fiber charges efficiently, but may change the filter's packing density or structure. Noninvasive radiation may, therefore, be preferred in future studies as a means of eliminating the fiber charge.

The electrical removal force on submicrometer-sized aerosol particles can be stronger than the mechanical removal force, if the fiber charge density is high. A dust-mist filtering facepiece with 4 times greater fiber charge than another facepiece of the same category was found capable of providing 5 times more protection than the other facepiece.

Aerosol penetration through electrically charged filtering facepieces increases with time. The corresponding decrease in respiratory protection should, therefore, be considered when heavily loaded filtering facepieces are used in the workplace. Normal wear incurs less change in performance than shown in this study. During normal breathing, the cyclic flow through the filter medium ranges from zero to a maximum

value with a corresponding range of aerosol penetration values, and, therefore, particles deposited. The total aerosol load in the filter medium will, in general, not correspond to the aerosol load at the average flowrate, and may be affected by the humidity inside the respirator.

ACKNOWLEDGEMENTS

The authors appreciate the financial support of the National Institute for Occupational Safety and Health through Grant No. R01-OH-01301. C.C. Chen was supported by a stipend for graduate education awarded by the University of Cincinnati during part of his Ph.D. study. The authors also thank Frank Platek and associates of the Applied Biology and Physics Branch, NIOSH - Cincinnati, for providing scanning electron microscopic pictures of the filters used.

REFERENCES

1. **Chen, C.C., M. Lehtimäki, and K. Willeke:** Aerosol Penetration through Filtering Facepieces and Cartridges. *Am. Ind. Hyg. Assoc. J. 53*:566–574 (1992).
2. **Brown, R.C.:** Modern Concepts of Air Filtration Applied to Dust Respirators. *Ann. Occup. Hyg. 33*: 615-644 (1989).
3. **Yeh, H.C. and B.Y.H. Liu:** Aerosol Filtration by Fibrous Filters-I. Theoretical. *J. Aerosol Sci. 5*: 191-204 (1974).
4. **Yeh, H.C. and B.Y.H. Liu:** Aerosol Filtration by Fibrous Filters II. Experimental. *J. Aerosol Sci. 5*: 205-217 (1974).
5. **Nguyen, X. and J.M. Beeckmans:** Single Fiber Capture Efficiencies of Aerosol Particles in Real and Model Filters in the Inertial- Interceptive Domain. *J. Aerosol Sci. 6*: 205-212 (1975).
6. **Ingham, D.B.:** The Diffusional Deposition of Aerosols in Fibrous Filter. *J. Aerosol Sci. 12*: 357-365 (1981).
7. **Lee, K.W. and B.Y.H. Liu:** Theoretical Study of Aerosol Filtration by Fibrous Filter. *Aerosol Sci. Technol. 1*: 147-161 (1982).
8. **Davies, C.N.:** Filtration of Aerosols. *J. Aerosol Sci. 14*: 147-161 (1983).
9. **Kirsch, A.A. and P.V. Chechuev:** Diffusion Deposition of Aerosol in Fibrous Filters at Intermediate Peclet Numbers. *Aerosol Sci. Technol. 4*: 11-16 (1985).
10. **Rao, N. and M. Faghri:** Computer Modeling of Aerosol Filtration by Fibrous Filters. *Aerosol Sci. Technol. 8*: 133-156 (1988).
11. **Lathrache, R., H.J. Fissan, and S. Neumann:** Deposition of Submicron Particles on Electrically Charged Fibers. *J. Aerosol Sci. 17*: 446-449 (1986).
12. **Kanaoka, C., H. Emi, Y. Otani, and T. Iiyama:** Effect of Charging State of Particles on Electret Filtration. *Aerosol Sci. Technol. 7*: 1-13 (1987).
13. **Emi, H., C. Kanaoka, Y. Otani, and T. Ishiguro:** Collection Mechanisms of Electret Filter. *Particulate Sci. and Technol. 5*: 161-171 (1987).
14. **Pich, J., H. Emi, and C. Kanaoka:** Coulombic Deposition Mechanism in Electret Filters. *J. Aerosol Sci. 18*: 29-35 (1987).
15. **Baumgartner, Hp. and F. Löffler:** A Basic Theoretical and Experimental Study of Particle Collection in Electret Fibre Filters. *Proc. Fourth World Filtration Congress.* Ostende, Belgium: 1986. pp 2.11-2.22.
16. **Lathrache, R. and H.J. Fissan:** Enhancement of Particle Deposition in Filters due to Electrostatic Effects. *Proc. of the Filtration Society* 418-422 (1987).
17. **Blackford, D.B., G.J. Bostock, R.C. Brown, R. Loxley, and D. Wake:** Alteration in the Performance of Electrostatic Filters Caused by Exposure to Aerosols. *Proc. Fourth World Filtration Congress.* Ostende, Belgium: 1986. pp 7.27-7.33.
18. **Brown, R.C., D. Wake, R. Gray, D.B. Blackford, and G.J. Bostock:** Effect of Industrial Aerosols on the Performance of Electrically Charged Filter Material. *Ann. Occup. Hyg. 32*: 271-294 (1988).
19. **Kanaoka, C., H. Emi, and T. Ishiguro:** Time Dependency of Collection Performance of Electret Filter. In *Aerosols.* New York: Elsevier Science Publishing Co., Inc., 1984. pp. 613-616.
20. **Hinds, W.C.:** *Aerosol Technology.* New York: John Wiley and Sons, Inc., 1982. pp. 164-186.
21. **Chen, C.C., J. Ruuskanen, W. Pilacinski, and K. Willeke:** Filter and Leak Penetration of a Dust and Mist Filtering Facepiece. *Am. Ind. Hyg. Assoc. J. 51*: 632-639 (1990).
22. **Pilacinski, W., C.C. Chen, and K. Willeke:** Size-Fractionating Aerosol Generator. *Aerosol Sci. Technol. 13*: 450-458 (1990).
23. **Pilacinski, W., K.W. Szewczyk, M. Lehtimäki, and K. Willeke:** Characteristics of a Double-Orifice Nebulizer. *J. Aerosol Sci. 21*: 977-982 (1990).
24. **Brown, R.C.:** A Many-Fiber Model of Airflow through a Fibrous Filter. *J. Aerosol Sci. 15*: 583-593 (1984).
25. **Ingham, D.B., P.J. Heggs, and M.L. Hildyard:** A Note on the Pressure Drop across a Fibrous Filter Modifier as a Symmetrical Array of Cylinders. *J. Aerosol Sci. 19*: 385-386 (1988).
26. "Mineral Resources," Code of Federal Regulations Title 30, Part 11: page 18-82 (1989).
27. **Liu, B.Y.H. and K.L. Rubow:** Air Filtration by Fibrous Midia. In *Fluid Filtration: Gas, Volume I.* R.R. Raber, ed. ASTM STP 975, 1986. pp 1-13.